

Lennart Karstensen*, Torben Pätz, Franziska Mathis-Ullrich and Jan Stallkamp

Facile Testbed for Robotic X-ray based Endovascular Interventions

Abstract: Endovascular surgical robotics requires a facile and realistic testbed to validate control algorithms. This work compares methods to manufacture such a testbed. Utilizing animal tissue, a mannequin, and a low-voltage flow pump it is possible to perform catheter-based interventions with X-ray feedback for less than €300. The aim of this paper is to lower the entry hurdle for validating endovascular surgical robots by providing a method to build a facile and low-budget testbed.

Keywords: endovascular, surgical robotics, testbed, X-ray, catheter

<https://doi.org/10.1515/cdbme-2021-1026>

1 Introduction

Endovascular interventions are the state-of-the-art treatment of many cardiovascular diseases. This category of diseases is the main cause of death worldwide (31.5%), in particular ischemic heart (14.8%) and cerebrovascular (11.7%) disease [1]. In developed countries, the number of cases tends to increase because of the aging population and increasing incidence of obesity. Assistance in the form of endovascular robotics can be a key factor in ensuring the provision of medical care in the future.

Research on endovascular surgical robots requires a reproducible method to perform interventions for development and testing. Simulation models are sufficient for proof-of-concepts and basic development, but a significant gap between simulation and reality still exists. This raises the need for realistic testbeds, which reduce the gap to human trials. The

Table 1: Overview of testbeds used in autonomous endovascular robotics

Author	Material	Anatomy	Feedback
Karstensen [2]	Rigid Plastic	Technical	Camera Image
Chi [3]	Flexible plastic	Realistic	EM Tracking
Jayender [4]	Flexible plastic	Technical	EM Tracking
Ji [5]	Flexible plastic	Realistic	EM Tracking
Raffii-Tari [6]	Flexible plastic	Realistic	EM Tracking
Tercero [7]	Flexible plastic	Realistic	EM Tracking
Zhao [8]	Rigid plastic	Technical	Camera image
Schwein [9]	Rigid plastic	Realistic	X-ray Image

testbed should allow endovascular catheter navigation in arteries or veins with high repeatability and realistic X-ray image quality.

A large number of endovascular phantoms with good X-ray imaging quality already exists, e.g. Boltz et al. [10]. They are very well suited for the purpose they are built for, but typically neglect the mechanical properties necessary for endovascular catheter navigation. Table 1 provides an overview of testbeds utilized by researchers in the field of endovascular robotics. Mainly realistic anatomies made of flexible plastic with electromagnetic (EM) tracking are utilized. EM tracking has the advantages that the catheter position is given directly instead of extracting the position from an X-ray image, such that the researcher can concentrate on the catheter control algorithm. But this is a big obstacle for the implementation as there are no approved EM tracking systems available and adaption to X-ray feedback is necessary.

It is noticeable, that so far, no animal specimen has been used for validation of autonomous endovascular catheter navigation. The underrepresentation of X-ray based research for an intervention that is mainly performed using X-ray imaging in the standard of care, is presumably due to lack of access to an X-ray system, the increased difficulty of development due to radiation when using X-ray, and the increased effort to build a phantom with realistic X-ray imaging.

To mitigate the last reason, this work elaborates a facile and low-cost method to manufacture a testbed for endovascular interventions performed under X-ray imaging. Its main use case is testing of control algorithms for

*Corresponding author: Lennart Karstensen: Fraunhofer IPA, Project Group for Automation in Medicine and Biotechnology, Theodor-Kutzer-Ufer 1-3, 68167 Mannheim, Germany, e-mail: lennart.karstensen@ipa.fraunhofer.de

Torben Pätz: Fraunhofer Institute for Digital Medicine, Am Fallturm 1, 28359 Bremen, Germany

Franziska Mathis-Ullrich: Health Robotics and Automation, Institute for Anthropomatics and Robotics, Karlsruhe Institute of Technology, Engler-Bunte-Ring 8, Karlsruhe, Germany

Jan Stallkamp: Fraunhofer IPA, Project Group for Automation in Medicine and Biotechnology, Theodor-Kutzer-Ufer 1-3, 68167 Mannheim, Germany,

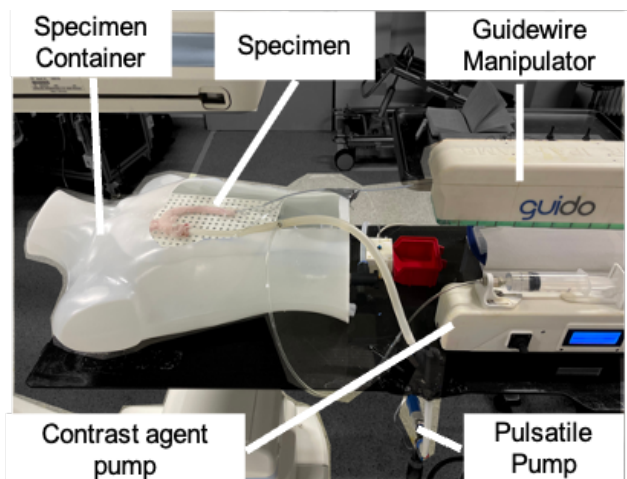


Figure 1: Final testbed with specimen, specimen container, pulsatile pump and syringe pump. The use-case is guidewire navigation by a telemanipulator with X-ray feedback.

autonomous catheter navigation with X-ray imaging, but it could also be utilized for training purposes or material testing.

2 Materials & Methods

The complete testbed is illustrated in Figure 1. It consists of a specimen, a specimen container, and a pulsatile pump. The testbed is utilized to navigate a guidewire in an aortic arch with a custom guidewire manipulator using X-ray fluoroscopy images as feedback (Artis Zeego, Siemens Healthcare GmbH, Germany) and a custom contrast agent pump similar to [11]. With this setup it is possible to perform catheter-based interventions with pulsatile blood flow, realistic fluoroscopic imaging, and the ability to visualize the vessel lumen using contrast agent. The specimen can be exchanged according to the current requirements.

Specimen

Different specimens can be categorized by vessel anatomy and material. For this testbed evaluation an aortic arch is the anatomy of choice as this is the most utilized anatomy for research in the field of catheter navigation. Three

different levels of realism are shown in Figure 2, namely a solid rigid material model, a tube-like elastic silicone phantom, and real ex-vivo tissue. They are compared regarding the manufacturing workload, long term stability of the resulting model, flexibility of different vessel anatomies, realism of the model, and cost.

For the solid rigid phantom, a vessel lumen mesh is extracted from a CT image with contrast agent injected in the vessel lumen. A CAD program is utilized to construct a solid body around the lumen mesh and the mesh is subtracted from the body. The final body is 3D printed using a stereolithography (SLA) printer (Form 3, Clear material, Formlabs Inc., USA). The tube-like elastic silicone phantom is a model that can be purchased. The ex-vivo tissue specimen is a porcine aorta obtained at the local abattoir. The aorta is dissected from the porcine heart and prepared by attaching hose nozzles to the open ends held in place by zip ties.

Specimen Container

A specimen container is necessary to embed the specimen in a surrounding medium with an X-ray density similar to soft tissue to obtain a realistic base image. For most use cases the X-ray density of water is sufficient. Additional structures can optionally be added to be visualized in the X-ray image, e.g., the rib cage. Here, several specimen containers are considered. Candidates include a custom aquarium-like container, a mannequin, and a large plastic box.

The applicability of the different specimen containers is compared regarding their resulting image quality. Hence, a porcine aorta is placed inside and attached to the pump and the contrast agent pump. A 500 g/l potassium iodide solution is injected with 1 ml/s in a constant blood flow of approximately 167 ml/s. To evaluate the imaging capabilities of the different testbeds, one fluoroscopic image without contrast agent and two consecutive CT scans with contrast agent are analyzed.

The fluoroscopic image is taken in the frontal plane and is rated for homogeneity and realism. The silicone tube on the left side, as seen in Figure 3, is neglected, as it is used only for the sake of a simple comparison of the images.



Figure 2: (A) CAD Model of solid phantom of a pig aorta. (B) United Biologics Silicone Aorta Phantom. (Image from United Biologics Inc.) (C) Porcine Aorta cut free. (D) Frontal Layer of the CT Image with measuring circles in the aortic arch, ascending aorta, and water

The CT scans are rated for technical image quality by analyzing the distribution of Hounsfield units (HU) at three different areas in the image, namely the aortic arch, the descending aorta and the surrounding water as shown in Figure 2D. Ideally, measurements in the aortic arch and ascending aorta are similar and present a distinct gap in HU to the surrounding water. The measurements should remain constant for both CT scans.

The plastic box is filled with water and the ex-vivo porcine aorta is placed inside and attached to the pulsatile pump and the contrast agent pump. The box has inner dimensions 200 x 300 x 100 mm (width x height x depth).

The mannequin is cut open and the base is sealed using silicone. The ex-vivo porcine aorta is attached to a perforated plate and connected to the pulsatile pump and the contrast agent pump. The mannequin has the dimensions 270-330 x 455-570 x 100 mm (width x height x depth).

The aquarium is custom made from plexiglass sheets. The sheets are cut, glued, and additionally sealed with silicone. The size of the aquarium is fit to the table for maximum flexibility. It has the dimensions 440 x 500 x 154 mm (width x height x depth).

For comparison, the reconstruction volume of the CT image can be approximated as cylinder with the dimensions $\varnothing 250$ mm x 184 mm. The diameter extends in the width and depth dimensions of the containers and the cylinder height corresponds to the container height.

Pulsatile Pump

Pulsatile simulated blood flow enables endovascular robot validation in a realistic environment, as the blood flow can impact catheter motion behavior. Additionally, simulated blood flow can be necessary to enable catheter navigation, e.g., to inflate real tissue arteries or veins.

The pulsatile pump is manufactured using a low-voltage flow pump (1395.79.59, Comet Pumps, USA) with a supply voltage of 24 V, a maximum output of 600 l/h and a maximum pressure of 0.55 bar. It is controlled by a microcontroller (Arduino Mega, Arduino, USA) with a motor driver (G2 High-Power Motor Driver 24v21, Pololu Corporation, USA). Pressure is measured with an integrated analog pressure sensor (ABPDANT005PGAA5, Honeywell International Inc., USA).

The pulsatile pump is controlled by a pulse duration modulation pattern, where the pump is switched on for a specified amount of time per pulse and switched off for the remaining time. The pump is adjusted to 80 pulses per minute (1.333 pulses per second) and a pulse width of 150 ms (150 ms on, 600 ms off).

The resulting blood pressure curve is compared to realistic pressure gradients. From [12] a physiological pressure rise of 547 mbar/s and fall of -197 mbar/s can be extracted.

Table 2: Overview of the characteristics of the different vessel specimen modes

Material	Manufac turing	Long Term Stability	Flexibility	Realism	Cost
Solid Rigid Material	-	+	+	-	0
Tube-like Elastic Material	+	+	-	0	-
Real Tissue	0	-	0	+	+

3 Results

The authors' choice for each component is summarized in Figure 1. To achieve the most realistic CT imaging results, the ex-vivo porcine aorta as a specimen is placed in a mannequin as specimen container.

Specimen

An overview of the characteristics of the different specimens is shown in Table 2.

The solid phantom has the advantage of high flexibility because models can be freely engineered and modified from CT data and the resulting vessel phantom is mechanically robust. The price is still moderate and is mainly caused by the SLA printing material. Disadvantage is the comparably high manufacturing time as the phantom must be engineered, printed and post-processed. Furthermore, the rigid, synthetic surface of the model is simplified compared to real blood vessels. Printing a phantom using stereolithography costs about €85 if a printer is available or €413 if commercially obtained (e.g., at rapidobject.com).

The advantage of the tube-like silicone model is the reduced manufacturing workload as the part is purchased as well as its long-term stability. The model is more realistic than a solid model, but the characteristics of the vessel surface still differ from real tissue. Disadvantages of this model are the reduced flexibility as the variety offered by the suppliers is limited and the high cost compared to the other materials. A model costs approximately €2000 (\$2520, United Biologics Inc.).

Real ex-vivo tissue has the advantage of high flexibility regarding vessel geometries, high realism and cost-effectiveness. The time for manufacturing is average, mainly attributed by dissecting the aorta from the porcine heart. The disadvantages are the reduced flexibility regarding pathologic structures as only healthy organs are offered by the abattoir

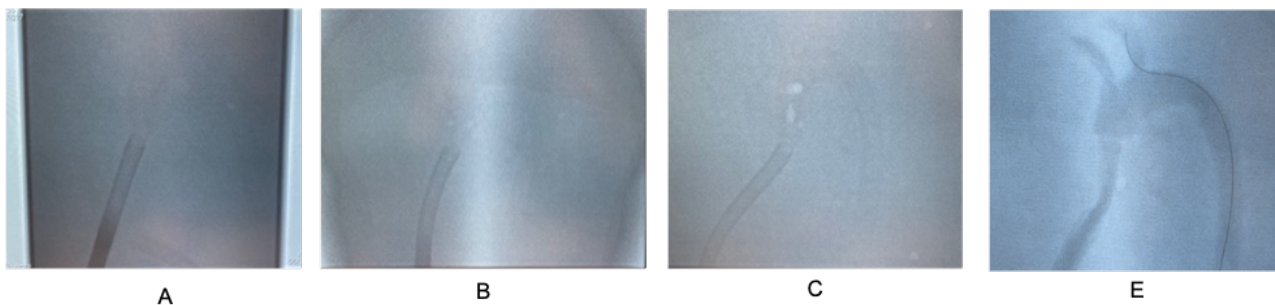


Figure 3: Fluoroscopy images of (A) the plastic box, (B) the mannequin, (C) the aquarium and (D) the mannequin with a guidewire inserted and contrast agent in the aorta.

and the reduced long-term stability of the model as the real tissue rapidly disintegrates at room temperature. However, for multiple uses the tissue can be frozen in between experiments. A porcine heart costs approximately €2 at the abattoir. To ensure to get at least one intact aorta, best practice is to purchase three or more hearts. At least one out of three hearts had incisions in the aorta rendering it useless. Therefore, one model costs about €6.

Specimen Container

The resulting fluoroscopic images are shown in Figure 3 and the HU distributions of the CT images in Figure 4.

The fluoroscopic image of the plastic box is sufficiently homogenous at the area of interest around the specimen. The container wall is visible as a sharp edge. The plastic box proves high CT image quality, the HU of the aortic arch and ascending aorta are similar in the same CT image and present a distinctive gap to the HU of water. A disadvantage is the different impact of contrast agent on both CT images. An increase in overall HU is visible in the second CT scan. Total cost for the container is about €10.

The fluoroscopic image of the mannequin has a mediocre homogeneity, but the inhomogeneities appear at the same location as they would in real patients. The container wall is only blurred visible. This container presents a good CT image

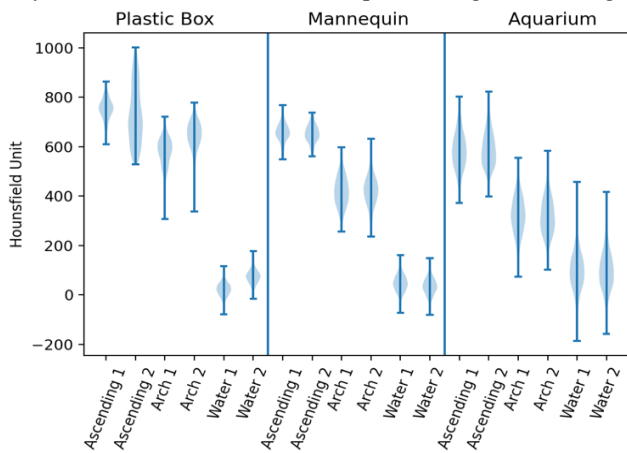


Figure 4: Distribution of Hounsfield units (HU) in the measurement circles in the CT slice at three different locations and two consecutive CTs for each specimen container

quality, the difference in HU between the aortic arch and the ascending aorta is larger than for the plastic box, but a gap to the water HU levels is still clearly visible. The HU for both CT scans remains stable. Total cost is about €25 for mannequin and silicone.

The fluoroscopic image of the aquarium has a high quality as it is very homogenous throughout the image. The CT image quality is relatively poor as the distribution of HU is widespread and there is a serious overlap between the HU distributions in water and the aorta. The HU for both CT scans stays stable. Total cost is approximately €420 for PMMA (Polymethylmethacrylat) sheets and glue.

Pulsatile Pump

The resulting pressure curve is presented in Figure 5. The pressure curve shows a delay of 59 ms and rises with a maximum rate of 122 mbar/s. After the pump is turned off, the pressure decreases with a delay of 41 ms and an initial rate of -107 mbar/s.

The resulting pulsatile blood flow is sufficient to visibly influence the movement of the guidewire during navigation. The pulsatile movement of the aorta and contrast agent injected into the aorta seem realistic upon visual inspection.

The complete setup for a pulsatile pump costs less than €100.

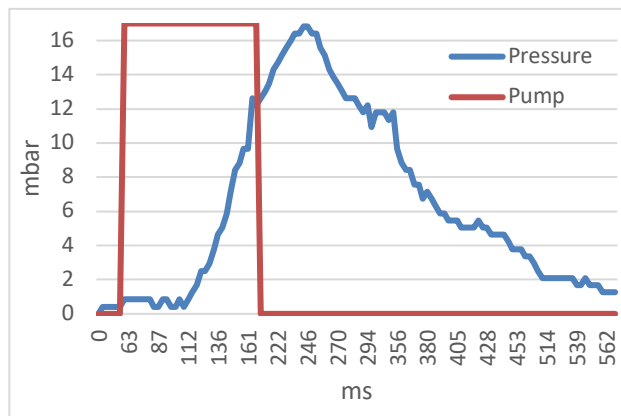


Figure 5: Pressure curve of the pulsatile pump at 80 bpm and 150ms on time per beat.

4 Discussion & Conclusion

In this work, methods to build a testbed for endovascular interventions are compared. The combination of a mannequin, porcine aorta, and low voltage pump with a microcontroller allows for endovascular interventions in real tissue with pulsatile blood flow and realistic X-ray feedback for less than €300. The facile testbed can be used for endovascular surgical robots.

The utilized specimen depends mainly on the required application. For example, if trials shall be repeated over a long duration, specimens made of synthetic material are advantageous. But if realism and different physiological anatomical geometries are important, ex-vivo porcine entrails present the best choice.

The mannequin appears to be the best specimen container. The CT image quality is good, the fluoroscopic image sufficiently realistic and it is easily obtained and adjusted as specimen container. The smaller plastic box has a better CT image quality but, due to the small volume, contrast agent concentration rises quickly and influences the image quality. The aquarium has a very high fluoroscopic image quality but shows poor CT image quality. This is mainly caused by 2D images in sagittal orientations, as the mass of the aquarium outside of the 3D reconstruction volume influences these images but is not considered in the reconstruction.

The pulsatile pump utilizing a common flow pump controlled by a microcontroller is a suitable method to achieve pulsatile blood flow simulation. The achieved pressure gradients are below physiological requirements. However, the flow profile appears to be sufficiently realistic. A reason for the difference between pressure and flow realism is presumably the highly reduced flow resistance compared to in-vivo aortas as the aorta has openings to the surrounding medium instead of capillary beds. As the resulting flow is the main influence on the navigation behavior this method seems valid for research and early development of robotic system.

Author Statement

Research funding: This project is funded by the Ministry of Economics, Labor and Tourism Baden-Württemberg within the framework of the Forum Gesundheitsstandort Baden-Württemberg.

Conflict of interest: Authors state no conflict of interest.

References

[1] M. Naghavi *u. a.*, „Global, regional, and national age-sex specific all-cause and cause-specific mortality for 240 causes of

death, 1990-2013: A systematic analysis for the Global Burden of Disease Study 2013“, *The Lancet*, Bd. 385, Nr. 9963, S. 117–171, 2015, doi: 10.1016/S0140-6736(14)61682-2.

[2] L. Karstensen, T. Behr, T. P. Pusch, F. Mathis-Ullrich, und J. Stallkamp, „Autonomous guidewire navigation in a two dimensional vascular phantom“, *Curr. Dir. Biomed. Eng.*, Bd. 6, Nr. 1, S. 1–4, 2020, doi: 10.1515/cdbme-2020-0007.

[3] W. Chi *u. a.*, „Collaborative Robot-Assisted Endovascular Catheterization with Generative Adversarial Imitation Learning“, *Proc. - IEEE Int. Conf. Robot. Autom.*, S. 2414–2420, 2020, doi: 10.1109/ICRA40945.2020.9196912.

[4] J. Jayender, R. V. Patel, und S. Nikumb, „Robot-assisted active catheter insertion: Algorithms and experiments“, *Int. J. Robot. Res.*, Bd. 28, Nr. 9, S. 1101–1117, 2009, doi: 10.1177/0278364909103785.

[5] C. Ji, Z.-G. Hou, und X.-L. Xie, „Guidewire navigation and delivery system for robot-assisted cardiology interventions“, in *IEEE 10th International Conference on Cognitive Informatics and Cognitive Computing (ICCI-CC'11)*, Banff, AB, Canada, Aug. 2011, S. 330–335. doi: 10.1109/COGINF.2011.6016161.

[6] H. Rafii-Tari, C. Bicknell, und G. Yang, „Learning-Based Modeling of Endovascular Catheterization“, *Int. Conf. Med. Image Comput. Comput.-Assist. Interv.*, S. 369–377, 2013, doi: 10.1007/978-3-642-40763-5_46.

[7] C. Tercero *u. a.*, „Autonomous catheter insertion system using magnetic motion capture sensor for endovascular surgery“, *Int. J. Med. Robot.*, Bd. 3, Nr. 1, S. 52–58, März 2007, doi: 10.1002/rcs.116.

[8] Y. Zhao *u. a.*, „A CNN-based prototype method of unstructured surgical state perception and navigation for an endovascular surgery robot“, *Med. Biol. Eng. Comput.*, Bd. 57, Nr. 9, S. 1875–1887, 2019, doi: 10.1007/s11517-019-02002-0.

[9] A. Schwein *u. a.*, „Electromagnetic tracking of flexible robotic catheters enables “assisted navigation” and brings automation to endovascular navigation in an in vitro study“, *J. Vasc. Surg.*, Bd. 67, Nr. 4, S. 1274–1281, 2018, doi: 10.1016/j.jvs.2017.01.072.

[10] T. Boltz, W. Pavlicek, R. Paden, M. Renno, A. Jensen, und M. Akay, „An anthropomorphic beating heart phantom for cardiac X-ray CT imaging evaluation“, *J. Appl. Clin. Med. Phys.*, Bd. 11, Nr. 1, S. 191–199, Dez. 2010, doi: 10.1120/jacmp.v11i1.3129.

[11] B. Wijnen, E. J. Hunt, G. C. Anzalone, und J. M. Pearce, „Open-Source Syringe Pump Library“, *PLoS ONE*, Bd. 9, Nr. 9, S. e107216, Sep. 2014, doi: 10.1371/journal.pone.0107216.

[12] B. J. P. van der Ster, F. C. Bennis, T. Delhaas, B. E. Westerhof, W. J. Stok, und J. J. van Lieshout, „Support Vector Machine Based Monitoring of Cardio-Cerebrovascular Reserve during Simulated Hemorrhage“, *Front. Physiol.*, Bd. 8, S. 1057, Jan. 2018, doi: 10.3389/fphys.2017.01057.